J. Am. Chem. Soc. 1994, 116, 1941–1952

Layered Materials by Molecular Design: Structural Enforcement by Hydrogen Bonding in Guanidinium Alkane- and Arenesulfonates

Victoria A. Russell,[†] Margaret C. Etter,[†,§] and Michael D. Ward*,[‡]

Contribution from the Department of Chemistry, Smith Hall, 207 Pleasant Street SE, and
Department of Chemical Engineering and Materials Science, Amundson Hall,
421 Washington Avenue SE, University of Minnesota, Minneapolis, Minnesota 55455

Received October 22, 1993. Revised Manuscript Received December 6, 1993[⊗]

Abstract: Single crystal X-ray structures of a series of guanidinium alkane- and arenesulfonates $C(NH_2)_3{}^+RSO_3{}^-$ (R = $(CH_2)_xCH_3$ (x = 0–3), (1*S*)-(+)-10-camphor, benzene, 1-naphthalene, and 2-naphthalene) reveal self-assembly of the ions into unique two-dimensional hydrogen-bonded sheets directed by hydrogen bonds between the six guanidinium protons and the six lone electron pairs of the sulfonate oxygen atoms. The sheets assemble in the third dimension as either single layers or bilayers with interpenetrating R groups, depending upon the steric requirements of the R groups. The observed solid-state motifs demonstrate that guanidinium sulfonates represent a novel class of crystalline solids for the molecular-level design and synthesis of new electronic materials.

Introduction

Organic molecular materials often possess interesting electronic properties, including nonlinear optical behavior, electrical conductivity, superconductivity, and ferromagnetism.[1] The relationship between molecular structure, supramolecular structure, and these bulk crystal properties is still not fully understood, and study of structural control on a molecular level continues. Control of molecular orientation in supramolecular structure is difficult and is recognized as a major obstacle in materials design.[2] Many attempts to control the structure of solids have focused on crystal engineering via charge-transfer,[3] electrostatic,[4] and hydrogen-bonding interactions. Design of solid-state motifs in which self-assembly into preordained motifs is directed by hydrogen bonding has been especially noteworthy,[5] particularly in the synthesis of crystals for second harmonic generation (SHG).[6] The diverse variety of hydrogen-bonding functionalities, for example, carboxylic acids,[7] nitroanilines,[8] imides,[9] and diarylureas,[10] provides considerable design flexibility and has enabled the formulation of hydrogen-bond "rules"[11] as general guidelines for predicting hydrogen-bond patterns in molecular crystals. Of particular interest is the control of dimensionality provided by tailored hydrogen-bonding networks,[12] as dimensionality can be crucial for electronic properties such as nonlinear optical activity[1a] and electronic conduction.[1b]

Our interest in the rational design and synthesis of molecular crystals with controlled dimensionality prompted us to explore a new class of hydrogen-bonded salts based on guanidinium and organic sulfonate ions. Simple extension of hydrogen bonding rules suggested that these ions would not only interact strongly by (guanidinium)N—H···O(sulfonate) hydrogen bonds but would also assemble into ordered *two-dimensional* networks as a consequence of equal numbers of donor and acceptor hydrogen-bonding sites and a three-fold molecular topology common to both guanidinium and sulfonate ions. Coulombic forces between the oppositely charged ions would further enhance network formation. We presumed that solid-state optoelectronic properties, including SHG, could be manipulated by judicious choice of the sulfonate R group. We were particularly interested in determining whether the strength of hydrogen bonding operative in such networks could be exploited to overcome the tendency for materials to crystallize in centrosymmetric space groups,[13] in

---

[*] Author to whom correspondence should be addressed.

[†] Department of Chemistry.

[‡] Department of Chemical Engineering and Materials Science.

[§] Deceased June 10, 1992.

[⊗] Abstract published in *Advance ACS Abstracts,* February 1, 1994.

(1) (a) *Nonlinear Optical Properties of Organic Molecules and Crystals*; Chemla, D. S., Zyss, J., Eds.; Academic Press: Orlando, FL, 1987; Vol. 1. (b) *Extended Linear Chain Compounds*; Miller, J. S., Ed.; Plenum: New York, 1982–1983; Vols. 1–3.

(2) Desiraju, G. R. *Crystal Engineering: The Design of Organic Solids*; Elsevier: New York, 1989.

(3) Herbstein, F. H. In *Perspectives in Structural Chemistry*; Dunitz, J. D., Ibers, J. A., Eds.; Wiley and Sons: New York, 1971; Vol. 4, pp 166–395.

(4) (a) Ward, M. D.; Fagan, P. J.; Calabrese, J. C.; Johnson, D. C. *J. Am. Chem. Soc.* **1989**, *111*, 1719. (b) Fagan, P. J.; Ward, M. D.; Calabrese, J. C. *J. Am. Chem. Soc.* **1989**, *111*, 1698.

(5) For recent work on use of hydrogen bonding for designed structures, see: (a) Lehn, J.-M.; Mascal, M.; DeCian, A.; Fischer, J. *J. Chem. Soc., Perkin Trans. 2* **1992**, 461. (b) Lehn, J.-M.; Mascal, M.; DeCian, A.; Fischer, J. *J. Chem. Soc., Chem. Commun.* **1990**, 479. (c) Fouquey, C.; Lehn, J.-M.; Levelut, A.-M. *Adv. Mater.* **1990**, *2*, 254. (d) Zerowski, J. A.; Seto, C. T.; Whitesides, G. M. *J. Am. Chem. Soc.* **1992**, *114*, 5473. (e) Seto, C. T.; Whitesides, G. M. *J. Am. Chem. Soc.* **1991**, *113*, 712. (f) Whitesides, G. M.; Mathias, J. P.; Seto, C. T. *Science* **1991**, *254*, 1312. (g) Zerowski, J. A.; Seto, C. T.; Wierda, D. A.; Whitesides, G. M. *J. Am. Chem. Soc.* **1990**, *112*, 9025. (h) Seto, C. T.; Whitesides, G. M. *J. Am. Chem. Soc.* **1990**, *112*, 6409. (i) Persico, F.; Wuest, J. D. *J. Org. Chem.* **1993**, *58*, 95. (j) Simard, M.; Su, D.; Wuest, J. D. *J. Am. Chem. Soc.* **1991**, *113*, 4696. (k) Ducharme, Y.; Wuest, J. D. *J. Org. Chem.* **1988**, *53*, 5787. (l) Gallant, M.; Biet, M. T. P.; Wuest, J. D. *J. Org. Chem.* **1991**, *56*, 2284. (m) Scoponi, M.; Polo, E.; Pradella, F.; Bertolasi, V.; Carassiti, V.; Goberti, P. *J. Chem. Soc., Perkin Trans. 2* **1992**, 1127.

(6) (a) Etter, M. C.; Frankenbach, G. M.; Adsmond, D. A. *Mol. Cryst. Liq. Cryst.* **1990**, *187*, 25. (b) Etter, M. C.; Frankenbach, G. M. *Chem. Mater.* **1989**, *1*, 10.

(7) Frankenbach, G. M.; Etter, M. C. *Chem. Mater.* **1992**, *4*, 272.

(8) (a) Etter, M. C.; Huang, K. S. *Chem. Mater.* **1992**, *4*, 824. (b) Etter, M. C.; Huang, K. S.; Frankenbach, G. M.; Adsmond, D. A. In *Materials for Nonlinear Optics, Chemical Perspectives*; Marder, S. R., Sohn, J. E., Stucky, G. D., Eds.; ACS Symposium Series 455; American Chemical Society: Washington, DC, 1991; pp 446–455. (c) Panunto, T. W.; Urbánczyk-Lipkowska, Z.; Johnson, R.; Etter, M. C. *J. Am. Chem. Soc.* **1987**, *109*, 7786.

(9) (a) Reutzel, S. M.; Etter, M. C. *J. Phys. Org. Chem.* **1992**, *5*, 44. (b) Etter, M. C.; Reutzel, S. M. *J. Am. Chem. Soc.* **1991**, *113*, 2586.

(10) Etter, M. C.; Urbánczyk-Lipkowska, Z.; Zia-Ebrahimi, M.; Panunto, T. W. *J. Am. Chem. Soc.* **1990**, *112*, 8415.

(11) (a) Etter, M. C. *J. Phys. Chem.* **1991**, *95*, 4601. (b) Etter, M. C. *Acc. Chem. Res.* **1990**, *23*, 120.

(12) (a) Chang, Y.-L.; West, M.-A.; Fowler, F. W.; Lauher, J. W. *J. Am. Chem. Soc.* **1993**, *115*, 5991. (b) Lauher, J. W.; Chang, Y.-L.; Fowler, F. W. *Mol. Cryst. Liq. Cryst.* **1992**, *211*, 99. (c) Zhao, X.; Chang, Y.-L.; Fowler, F. W.; Lauher, J. W. *J. Am. Chem. Soc.* **1990**, *112*, 6627. (d) Hollingsworth, M. D.; Santansiero, B. D.; Oumar-Mahamat, H.; Nichols, C. J. *Chem. Mater.* **1991**, *3*, 23. (e) Garcia-Tellado, F.; Geib, S. J.; Goswami, S.; Hamilton, A. D. *J. Am. Chem. Soc.* **1991**, *113*, 9265.

(13) (a) Kitaigorodsky, A. I. *Molecular Crystals and Molecules*; Academic Press: New York, 1973. (b) Whitesell, J. K.; Davis, R. E.; Saunders, L. L.; Wilson, R. J.; Feagins, J. P. *J. Am. Chem. Soc.* **1991**, *113*, 3267.

0002-7863/94/1516-1941$04.50/0

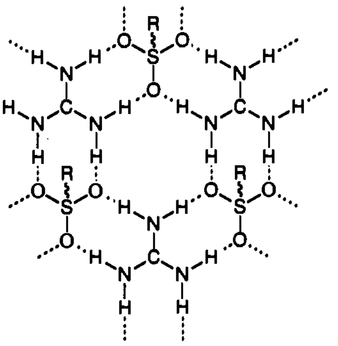

which SHG is forbidden.[14] In addition, strong intermolecular bonding in these networks may favor the formation of low-density solids that may be potentially useful as host lattices. The flexibility provided by ready substitution of the sulfonate R groups also suggested that synthesis of electronic conductors with structurally enforced two-dimensional character may be realized, which has been shown to be important in recent developments in organic superconductors.[15] Herein we describe the synthesis and characterization of our initial series of guanidinium sulfonate salts, containing simple alkane- and arenesulfonates. Their hydrogen-bonded networks, the role of the sulfonate R groups in crystal packing, and the implications of these findings for materials design are presented and discussed.

Experimental Section

Materials. All starting materials were purchased from the Aldrich Chemical Company and used as received. Spectroscopic-grade solvents and/or deionized water were used for all crystallizations.

Characterization. Melting points were determined by differential scanning calorimetry (DSC) on a Mettler FP80/FP84 (100 mV, 1 deg/min) and are uncorrected. Infrared spectra were recorded on a Nicolet 510M spectrometer (4-cm^{-1} resolution) as Nujol mulls. Solution 200-MHz ^{1}H NMR spectra were recorded on an IBM NR200AF spectrometer in $(CD_3)_2SO$ (Cambridge Isotope Laboratories) relative to internal standard TMS. Elemental analysis was obtained from M-H-W Laboratories, Phoenix, AZ.

Experimental details of the X-ray analysis of the salts presented here are given in Table 1. Single crystal X-ray structural data were collected at 24 °C on an Enraf-Nonius CAD4 diffractometer with graphite monochromated Mo Kα radiation (λ = 0.710 69). Lattice parameters were obtained from least-squares analysis of 23–25 reflections. Three standard reflections were measured every 50–60 min. All structures were corrected for Lorentz and polarization effects, and other corrections are noted in Table 1. Structures were solved by direct methods with MITHRIL[16] and DIRDIF.[17] All non-hydrogen atoms were refined anisotropically. Guanidinium N–H protons were refined with isotropic temperature factors for **1**–**3** and **7**–**9**. The range of temperature factors for each compound was, in Å^2, **1**, (3.3–10); **2**, (4.4–8); **3**, (4.9–7); **7**, (4–8); **8**, (5.2–10); and **9**, (3–11). The range of N–H distances for each compound was, in Å, **1**, (0.74–0.94); **2**, (0.80–0.90); **3**, (0.76–0.85); **7**, (0.77–0.99); **8**, (0.82–0.92); and **9**, (0.72–1.03). Other hydrogen atoms included in the structure factor calculations were placed in idealized positions (d_{C-H} = 0.95 Å, and for **5** and **6**, d_{N-H} = 0.95 Å) with assigned isotropic thermal parameters (B = 1.2B of bonded atoms).

Synthesis of Guanidinium Sulfonate Salts. Guanidinium sulfonates were prepared by slow evaporation of equimolar solutions of guanidine hydrochloride and the appropriate sulfonic acid or sodium or potassium sulfonate under ambient conditions. Crystals were removed from solution prior to total evaporation.

Guanidinium Methanesulfonate (1). Crystallized from water, methanol, or aqueous methanol solutions of guanidine hydrochloride/methanesulfonic acid as colorless hexagonal and trigonal plates: mp 206–207 °C; IR 3333, 3262, 3188, 2236, 1679, 1586, 1482, 1418, 1378, 1191, 1157, 1056, 780, 722 cm^{-1}; ^{1}H NMR δ 7.07 (s, 6 H, $[C(NH_2)_3]^+$), 2.43 (s, 3 H, $CH_3SO_3^-$). Anal. Calcd for $C_2H_9N_3O_3S$: C, 15.48; H, 5.85; N, 27.08; S, 20.67. Found: C, 15.74; H, 5.94; N, 27.27; S, 20.42.

Guanidinium Triflate (2). Crystallized from water or 1:1 methanol–acetonitrile solutions of guanidine hydrochloride/triflic acid as colorless hexagonal and trigonal plates: mp 156.5–157.5 °C; IR 3411, 3292, 3264, 3234, 2220, 1695, 1582, 1558, 1464, 1458, 1376, 1256, 1187, 1040, 766, 721, 648 cm^{-1}; ^{1}H NMR δ 6.92 (s, $[C(NH_2)_3]^+$). Anal. Calcd for $C_2H_6F_3N_3O_3S$: C, 11.49; H, 2.89; N, 20.09; S, 15.33. Found: C, 11.62; H, 2.65; N, 20.05; S, 15.45.

Guanidinium Ethanesulfonate (3). Crystallized from 3:1 acetonitrile–water solution of guanidine hydrochloride/ethanesulfonic acid as colorless hexagonal plates: DSC endotherms 106–107, 159–162 °C; IR 3359, 3334, 3260, 3191, 1681, 1584, 1459, 1410, 1378, 1295, 1245, 1183, 1160, 1046, 980, 783, 747, 722 cm^{-1}; ^{1}H NMR δ 6.99 (s, 6 H, $[C(NH_2)_3]^+$), 2.46 (q, 2 H, CH_3CH_2-), 1.08 (t, 3 H, CH_3CH_2-). Anal. Calcd for $C_3H_{11}N_3O_3S$: C, 21.30; H, 6.55; N, 24.83; S 18.95. Found: C, 21.41; H, 6.75; N, 24.96; S, 18.76.

Guanidinium 1-Propanesulfonate (4). Crystallized from 15:1 acetonitrile–water solution of guanidine hydrochloride/sodium 1-propanesulfonate monohydrate as very thin, colorless needles: mp 153–154 °C; IR 3361, 3338, 3261, 3195, 1681, 1584, 1463, 1416, 1378, 1299, 1252, 1218, 1187, 1048, 785, 722 cm^{-1}; ^{1}H NMR δ 6.99 (s, 6 H, $[C(NH_2)_3]^+$), 2.44–2.36 (m, 2 H, $CH_3CH_2CH_2SO_3^-$), 1.63–1.52 (sextet, 2 H, CH_3CH_2-$CH_2SO_3^-$), 0.90 (t, 3 H, $CH_3CH_2CH_2SO_3^-$). Anal. Calcd for $C_4H_{13}N_3O_3S$: C, 26.22; H, 7.15; N, 22.93; S 17.50. Found: C, 26.29; H, 7.36; N, 23.01; S, 17.66. Experimental density determined as ~1.18 g/cm^3 by flotation in *o*-nitrotoluene (d = 1.163 g/cm^3)/nitrobenzene (d = 1.196 g/cm^3).

Guanidinium 1-Butanesulfonate (5). Crystallized from 20:1 acetonitrile–water solution of guanidine hydrochloride/sodium 1-butanesulfonate as thin, colorless needles: mp 152–153 °C; IR 3371, 3330, 3261, 3185, 1677, 1586, 1461, 1378, 1308, 1279, 1241, 1206, 1165, 1046, 795, 724 cm^{-1}; ^{1}H NMR δ 6.99 (s, 6 H, $[C(NH_2)_3]^+$), 2.43 (~t, 2 H, $CH_3CH_2CH_2CH_2SO_3^-$), 1.55 (~quintet, 2 H, $CH_3CH_2CH_2CH_2SO_3^-$), 1.32 (sextet, 2 H, J = 7.3 Hz, $CH_3CH_2CH_2CH_2SO_3^-$), 0.85 (t, 3 H, J = 7.2 Hz, $CH_3CH_2CH_2CH_2SO_3^-$). Anal. Calcd for $C_5H_{15}N_3O_3S$: C, 30.44; H, 7.66; N, 21.30; S, 16.26. Found: C, 30.53; H, 7.44; N, 21.49; S, 16.09.

Guanidinium (1*S*)-(+)-10-Camphorsulfonate (6). Crystallized from 50% aqueous methanol solution of guanidine hydrochloride/(1*S*)-(+)-10-camphorsulfonic acid as colorless prisms: mp >300 °C; IR 3369, 3338, 3259, 3195, 2232, 1748, 1677, 1584, 1459, 1414, 1391, 1376, 1300, 1281, 1256, 1225, 1200, 1189, 1167, 1152, 1044, 967, 936, 853, 791, 766, 745, 652, 617 cm^{-1}; ^{1}H NMR δ 7.00 (s, 6 H, $[C(NH_2)_3]^+$), 2.91 (d, 1 H, -$CH(H)SO_3^-$), 2.42 (d, 1 H, -$CH(H)SO_3^-$), 2.73–1.28 (m, 7 H, camphor 3,4,5,6-H), 1.06 (s, 3 H, CH_3-), 0.76 (s, 3 H, CH_3-). Anal. Calcd for $C_{11}H_{21}N_3O_4S$: C, 45.34; H, 7.26; N, 14.42; S, 11.01. Found: C, 45.55; H, 7.43; N, 14.54; S, 11.05.

Guanidinium Benzenesulfonate (7). Crystallized from methanol solution of guanidine hydrochloride/benzenesulfonic acid as colorless needles: mp 208–210 °C; IR 3341 (3400–3341 br), 3258, 3186, 2222, 1678, 1663 (sh), 1582, 1462, 1445, 1377, 1194, 1158, 1154, 1127, 1069, 1035, 1019, 998, 921, 753, 730, 687 cm^{-1}; ^{1}H NMR δ 7.61 (m, 2 H, Ar-*H* ortho to SO_3), 7.34 (m, 3 H, Ar-*H* meta and para to SO_3), 6.98 (s, 6 H, $[C(NH_2)_3]^+$). Anal. Calcd for $C_7H_{11}N_3O_3S$: C, 38.70; H, 5.10; N, 19.34; S, 14.76. Found: C, 38.88; H, 5.30; N, 19.35; S, 14.63.

Guanidinium 1-Naphthalenesulfonate (8). Crystallized from 50% aqueous methanol solution of guanidine hydrochloride/sodium 1-naphthalenesulfonate as light tan needles: mp 277–278.5 °C; IR 3370, 3329, 3252, 3183, 1674, 1586, 1509, 1460, 1377, 1344, 1206, 1180 (sh), 1166 (sh), 1152, 1069, 1047, 969, 791, 762, 741, 721, 694 cm^{-1}; ^{1}H NMR δ 8.85–8.81 (m, 1 H, 2-*H*), 7.97–7.89 (m, 3 H, 4,5,8-*H*), 7.54–7.41 (m, 3 H, 3,6,7-*H*), 6.97 (s, 6 H, $[C(NH_2)_3]^+$). Anal. Calcd for $C_{11}H_{13}N_3O_3S$: C, 49.43; H, 4.90; N, 15.72; S, 12.00. Found: C, 49.65; H, 5.16; N, 15.83; S, 11.83.

Guanidinium 2-Naphthalenesulfonate (9). Crystallized from methanol solution of guanidine hydrochloride/2-naphthalenesulfonic acid as light

---

[14] (a) Zyss, J.; Oudar, J. L. *Phys. Rev.* **1982**, *A26*, 2016. (b) Oudar, J. L.; Zyss, J. *Phys. Rev.* **1982**, *A26*, 2028. (c) Zyss, J.; Chemla, D. S.; Nicoud, J. F. *J. Chem. Phys.* **1981**, *74*, 4800. (d) Zyss, J.; Nichoud, J. F.; Coquillay, M. *J. Chem. Phys.* **1984**, *81*, 4160. (e) Zyss, J.; Berthier, G. *J. Chem. Phys.* **1982**, *77*, 3635.

[15] (a) Inokuchi, H. *Angew. Chem., Int. Ed. Engl.* **1988**, *27*, 1747. (b) Montgomery, L. K.; Geiser, U.; Wang, H. H.; Beno, M. A.; Schultz, A. J.; Kini, A. M.; Carlson, K. D.; Williams, J. M.; Whitworth, J. R. *Synth. Met.* **1988**, *27*, A195. (c) Emge, T. J.; Leung, P. C. W.; Beno, M. A.; Wang, H. H.; Firestone, M. A.; Webb, K. S.; Carlson, K. D.; Williams, J. M.; Venturini, E. L.; Azevedo, L. J.; Schirber, J. E. *Mol. Cryst. Liq. Cryst.* **1986**, *132*, 363. (d) Williams, J. M.; Carneiro, K. *Adv. Inorg. Chem. Radiochem.* **1985**, *29*, 249.

[16] Gilmore, C. J. *J. Appl. Crystallogr.* **1984**, *17*, 42.

[17] Beurskens, P. T.; Bosman, W. P.; Doesburg, H. M.; Gould, R. O.; Van den Hark, Th. E. M.; Prick, P. A. J.; Noordik, J. H.; Beurskens, G.; Parthasarathi, V.; Bruins Slot, H. J.; Haltiwanger, R. C. DIRDIF: Direct Methods for Difference Structures. Technical Report 1984/1; Crystallography Laboratory: Toernooiveld, 6525 Ed Nijmegen, The Netherlands, 1984.

Table 1. Crystallographic Data for Guanidinium Sulfonates **1–3** and **5–9**

	compound							
	1	**2**	**3**	**5**	**6**	**7**	**8**	**9**
(A) Crystal Parameters								
formula	$C_2H_9N_3O_3S$	$C_2H_6F_3N_3O_3S$	$C_3H_{11}N_3O_3S$	$C_5H_{15}N_3O_3S$	$C_{11}H_{21}N_3O_4S$	$C_7H_{11}N_3O_3S$	$C_{11}H_{13}N_3O_3S$	$C_{11}H_{13}N_3O_3S$
FW	155.17	209.14	169.20	197.26	291.36	217.24	267.30	267.30
crystal size (mm^3)	0.70 × 0.50 × 0.10	0.55 × 0.45 × 0.15	0.55 × 0.45 × 0.17	0.55 × 0.25 × 0.15	0.63 × 0.45 × 0.45	0.70 × 0.30 × 0.15	0.60 × 0.20 × 0.15	0.60 × 0.15 × 0.10
space group	*C*2/*m*	*C*2/*c*	*C*2/*m*	*Pbcn*	$P2_1$	$P2_1/c$	*Pnma*	$P2_1/c$
crystal system	monoclinic	monoclinic	monoclinic	orthorhombic	monoclinic	monoclinic	orthorhombic	monoclinic
a (Å)	12.778(5)	12.988(7)	12.793(4)	14.733(4)	7.604(5)	7.50(1)	21.429(8)	7.495(6)
b (Å)	7.342(2)	7.512(2)	7.398(5)	12.278(4)	10.466(6)	23.287(6)	7.386(3)	28.349(6)
c (Å)	9.998(2)	18.45(1)	11.172(3)	12.314(7)	9.296(2)	12.060(2)	8.074(3)	12.040(3)
β (deg)	126.96(2)	111.69(4)	128.060(2)	90	90.66(4)	92.24(8)	90	91.29(5)
V (Å^3)	749.6(8)	1672(3)	833(1)	2228(2)	740(1)	2104(4)	1278(1)	2558(3)
Z	4	8	4	8	2	8	4	8
d_{calcd} (g/cm^3)	1.375	1.661	1.350	1.176	1.308	1.372	1.389	1.388
F (000)	328	848	360	848	312	912	560	1120
μ (Mo Kα) (cm^{-1})	3.66	3.99	3.35	2.59	2.22	2.82	2.45	2.45
(B) Data Collection								
scan technique	$\omega - 2\theta$	ω	$\omega - 2\theta$	ω	$\omega - 2\theta$	ω	ω	ω
$2\theta_{max}$ (deg)	51.9	51.9	56.0	47.9	51.9	48.0	52.0	48.0
data collected (*hkl*)	±15, +9, ±12	±12, +7, ±17	±16, +9, ±14	±13, +12, +15	±9, ±12, ±11	±8, +26, ±13	±9, +9, +26	±8, +32, ±13
scan speed (deg/min in ω)	4.1	2.1 to 16.5	8.2	1.0 to 16.5	16.5	16.5	8.2	4.1
reflections collected	1582	3126	2158	3826	5639	4743	2756	5015
unique reflections	793	1775	1083	2013	2913	3403	1491	4123
R(merg) (%)	4.9	3.8	8.6	6.6	3.9	4.2	3.9	5.1
corrections applied[a]	1, 2	1, 2	1, 2		1	2	2	2
(C) Refinement								
$R(F)^b$ (%)	5.1	3.8	5.8	5.6	3.7	5.3	4.9	4.8
$R(wF)^c$ (%)	7.9	5.3	7.2	5.1	4.5	5.8	5.0	4.8
Δ/σ (max)	0.02	0.04	0.02	0.01	0.00	0.06	0.03	0.05
$\Delta(\rho)$ (e$^-$/Å^3)	0.48	0.28	0.33	0.19	0.15	0.23	0.24	0.20
indep refl obs $F_o > 2\sigma(F_o)$	743	1284	749	833	2479	2039	866	2259
N_o/N_v	12.59	9.58	11.01	7.64	14.58	6.75	7.53	6.04
GOF	2.33	1.36	1.50	1.36	1.13	1.27	1.53	1.42

[a] All structures were corrected for Lorentz and polarization effects. 1 = empirical absorption using DIFABS (Walker, N.; Stuart, D. *Acta Crystallogr.* **1983**, *A39*, 158–166); 2 = secondary extinction. [b] $R(F) = \sum\|F_o| - |F_c\|/|F_o|$. [c] $R(wF) = [(\sum w(|F_o| - |F_c|)^2/\sum wF_o^2)]^{1/2}$; $w = 4F_o^2/\sigma^2(F_o)^2$.

gray-brown needles: mp 267–268 °C; IR 3370, 3335, 3256, 3186, 2222, 1677, 1665 (sh), 1582, 1462, 1377, 1347, 1273, 1205 (sh), 1189, 1156, 1138, 1093, 1036, 967, 955, 943, 909, 901, 867, 817, 754, 722, 678, 645 cm^{-1}; ^{1}H NMR δ 8.17 (s, 1 H, 1-*H*), 8.02–7.88 (m, 3 H, 4,5,8-*H*), 7.72 (dd, 1 H, J_1 = 8.6 Hz, J_2 = 1.6 Hz, 3-*H*), 7.70–7.52 (m, 2 H, 6,7-*H*), 6.99 (s, 6 H, $[C(NH_2)_3]^+$). Anal. Calcd for $C_{11}H_{13}N_3O_3S$: C, 49.43; H, 4.90; N, 15.72; S, 12.00. Found: C, 49.53; H, 5.00; N, 15.68; S, 12.13.

Results

Molecular Structures. An entire family of guanidinium sulfonate crystals can be grown simply by slow evaporation from various solvents under ambient conditions. These salts crystallize in either monoclinic or orthohombic space groups (Table 1). ORTEP views of the asymmetric units and atom labeling are given in Figure 1. No unusual trends in the intramolecular guanidinium C–N and sulfonate S–O bond lengths and angles were observed (Table 2). The nearly equivalent C–N and S–O bond lengths in the respective ions indicate that the electrons in both guanidinium and sulfonate groups are essentially delocalized. One noted exception is **1**, in which the guanidinium ion appears to have asymmetric bonding character, with one shorter C–N distance of 1.31 Å and two longer distances of 1.35 Å. The average C–N length observed overall was 1.32 Å, the N–C–N angle, 120.0°, the S–O length, 1.45 Å, and the O–S–O angle, 112.4°. The C–N lengths compare favorably with those found in a data base study[18] of bond lengths for unsubstituted guanidinium ion (mean C–N bond length 1.321 ± 0.008 Å). The experimental C–N bond lengths in guanidinium sulfonates also agree with theoretical C–N lengths of 1.321 and 1.334 Å.[19] The geometries of the sulfonate groups compare well with those found in other sulfonate structures. Other intramolecular bond lengths and angles for guanidinium sulfonates reported here are available as supplementary material.

Hydrogen Bonding in Guanidinium Sulfonates. Hydrogen bonding provides the major driving force for crystal packing in guanidinium sulfonates. In the following discussions, hydrogen-bond length refers to the N···O distance ($d_{N\cdots O}$) and hydrogen-bond angle to the N—H···O angle ($\theta_{N—H\cdots O}$). Evidence for an X—H···Y hydrogen bond is generally based on a X···Y distance that is less than the sum of the van der Waals radii of these atoms (for N—H···O hydrogen bonds, $d_{N\cdots O}$ = 3.07 Å[20]), assuming a linear X—H···Y angle, $\theta_{X—H\cdots Y}$. All hydrogen bonds in **1–3** and **5–9** fall within the distance criterion, ranging in $d_{N\cdots O}$ length from 2.86 to 3.06 Å (av 2.94 Å), but deviate from linearity, with $\theta_{N—H\cdots O}$ values ranging from 150.8 to 178.5° (av 168.1°) (Table 3). The $\theta_{N—H\cdots O}$ angles for **1–3** and **7–9** were determined from isotropically refined guanidinium hydrogen atom positions. In **5** and **6** the guanidinium hydrogens were placed in idealized positions, and there is more uncertainty in the $\theta_{N—H\cdots O}$ angles for these compounds. Nonlinear hydrogen bonds generally result from crystal packing forces, presumably from interactions between sulfonate R groups that reside between hydrogen-bonded layers.

Each individual pair of N—H···O interactions shown in **I** in Chart 1 can be characterized as a *dimer* formed via two amino

---

[18] Allen, F. H.; Kennard, O.; Watson, D. G.; Brammer, L.; Orpen, A. G.; Taylor, R. *J. Chem. Soc., Perkin Trans. 2* **1987**, S1.

[19] Gobbi, A.; Frenking, G. *J. Am. Chem. Soc.* **1993**, *115*, 2362.

[20] Bondi, A. *J. Phys. Chem.* **1964**, *68*, 441.

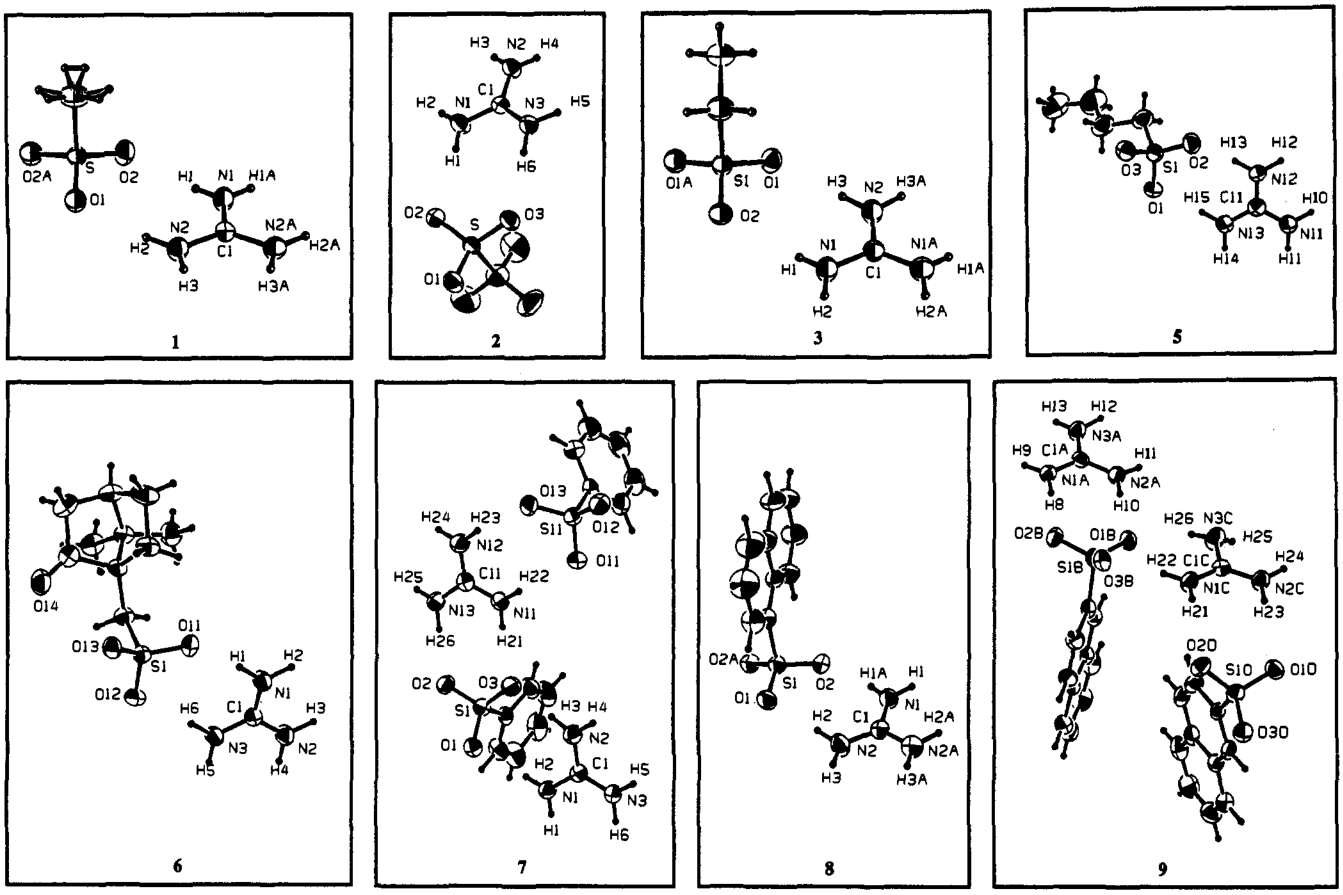

Figure 1. ORTEP drawings (30% probability ellipsoids) of asymmetric units and atom numbering schemes of guanidinium sulfonates. Hydrogen-bonded ribbon direction is approximately horizontal in each drawing. Note that in **1**, the methyl hydrogens are disordered over two positions.

protons on two nitrogen atoms of a single guanidinium ion and two lone electron pairs on two oxygen atoms of a sulfonate ion (i.e., eight-membered ring, graph set[21] motif $R_2^2(8)$). Three dimer interactions for each guanidinium and sulfonate ion comprise a hydrogen-bonded *sheet*, **III**. The sheet can also be described as hydrogen-bonded *ribbons*, **II**, linked into sheets **III** through $R_2^2(8)$ dimer interactions and $R_6^3(12)$ rings. Table 3 lists hydrogen-bond geometries and symmetry relations between ions and separates the hydrogen-bonding interactions as two dimers (A and B) linked into ribbons **II** (intraribbon) and linkage of ribbons into sheets **III** through dimer C interactions (interribbon). For ease of analysis (three possible ribbon choices run through each guanidinium ion), ribbon orientations are taken to be the most planar ribbon (as determined by coplanarity of the guanidinium ion with the sulfonate oxygen plane), those formed by mirror symmetry, or those most easily compared with other structures. These ribbon assignments are discussed later in this section and are listed by intraribbon symmetry operators in Table 3. Note that the ribbon direction is approximately in the plane of the paper and horizontal in the views of asymmetric units in Figure 1. The planarity of the hydrogen-bonded sheets can be characterized by an interribbon dihedral angle, θ_{IR}[22] (see equivalent drawing of **III** in Chart 1 and Table 3). An θ_{IR} of 180° represents the ideally planar hydrogen-bonded sheet. In actual crystal structures, this angle deviates from 180°, as ribbons are not coplanar due to crystal packing forces.

Guanidinium methanesulfonate (**1**) and guanidinium ethanesulfonate (**3**) are isostructural, each crystallizing into the $C2/m$ space group and containing half an ion pair per asymmetric unit with mirror symmetry imposed on the molecules. Hydrogen-bonded dimers form ribbons, generated by mirror symmetry, parallel to the *b*-axes. Hydrogen bonds within the ribbon in **1** are shorter ($d_{N\cdots O}$ = 2.92 and 2.89 Å) and protrude further from the plane of the ribbon ($\theta_{N-H\cdots O}$ = 168.2 and 160.6°) than those in **3** ($d_{N\cdots O}$ = 2.93 and 2.96 Å, $\theta_{N-H\cdots O}$ = 178.2 and 167.9°). Neighboring, *C*-center related ribbons are linked into hydrogen-bonded sheets parallel to (001) planes by $d_{N\cdots O}$ distances of 2.94 and 2.96 Å, $\theta_{N-H\cdots O}$ angles of 158.3 and 159.6°, and θ_{IR} angles of 171 and 170° for **1** and **3**, respectively. This nonlinearity of the interribbon hydrogen bonds results in slight puckering of hydrogen-bonded sheets. The hydrogen-bonded sheet is a quasihexagonal net with three-fold symmetry (Figure 2). The morphology of **1** reflects this symmetry, crystallizing as either hexagonal or trigonal shaped plates (Figure 3). The large hexagonal faces have been indexed as the (001) and (00$\bar{1}$) planes, corresponding to the planes of hydrogen bonding. Guanidinium triflate (**2**) crystallizes in a slightly different structure with hydrogen bonding in ribbons formed by *C*-center-related ions parallel to the *b*-axis. The nearly planar ribbons (average $\theta_{N-H\cdots O}$ = 174.2°) are linked into sheets parallel to (001) planes by nearly linear hydrogen bonding ($\theta_{N-H\cdots O}$ = 175.5 and 173.5°), with an interribbon dihedral angle, θ_{IR} of 163°. All hydrogen-bond lengths in **2** are equivalent within experimental error ($d_{N\cdots O}$ = 2.99 Å) and are slightly longer than those observed in other structures.

Guanidinium 1-butanesulfonate (**5**) possesses hydrogen-bonded ribbons, parallel to the [01$\bar{1}$] direction, formed between glide-related ions. These ribbons link with neighboring 2_1-screw-related ribbons to form rippled hydrogen-bonded "sheets". The $\theta_{N-H\cdots O}$ hydrogen-bond angles in this structure average 163.2°, with the greatest deviation from linearity being 153.7° (note that hydrogen

---

[21] Graph set analysis is a method of categorizing hydrogen-bond motifs based on graph theory. A graph set is designated using the pattern designator (G), its degree (r), and the number of donors (d) and acceptors (a), as shown: $G_d^a(r)$. G is a descriptor referring to the pattern of hydrogen bonding and has four different assignments: S (self), C (chain), R (ring), and D (dimer or discrete). Etter, M. C.; MacDonald, J. C.; Bernstein, J. *Acta Crystallogr.* **1990**, *B46*, 256.

[22] The interribbon dihedral angle, θ_{IR}, is the angle between the mean planes of one ribbon and its symmetry-related adjacent ribbon within a hydrogen-bonded sheet.

Table 2. Selected Intramolecular Bond Lengths and Angles for **1**–**3** and **5**–**9**

compound		C–N length (Å)		N–C–N angle (deg)		S–O length (Å)		O–S–O angle (deg)
1	C1–N1	1.312(5)	N1–C1–N2	119.4(1)	S1–O1	1.450(3)	O1–S1–O2	112.69(9)
	C1–N2	1.349(2)	N1–C1–N2A	119.4(1)	S1–O2	1.442(2)	O1–S1–O2A	112.69(9)
	C1–N2A	1.349(2)	N2–C1–N2A	121.2(3)	S1–O2A	1.442(2)	O2–S1–O2A	112.6(2)
2	C1–N1	1.321(3)	N1–C1–N2	119.8(3)	S–O1	1.439(2)	O1–S–O2	114.4(1)
	C1–N2	1.313(3)	N1–C1–N3	119.6(2)	S–O2	1.438(2)	O1–S–O3	114.5(1)
	C1–N3	1.320(3)	N2–C1–N3	120.5(3)	S–O3	1.442(2)	O2–S–O3	114.3(1)
3	C1–N1	1.312(3)	N1–C1–N1A	120.8(4)	S1–O1	1.446(2)	O1–S1–O1A	112.2(2)
	C1–N1A	1.312(3)	N1–C1–N2	119.6(2)	S1–O1A	1.446(2)	O1–S1–O2	112.3(1)
	C1–N2	1.328(5)	N1A–C1–N2	119.6(2)	S1–O2	1.452(3)	O1A–S1–O2	112.3(1)
5	C11–N11	1.324(7)	N11–C1–N12	120.7(7)	S1–O1	1.460(4)	O1–S1–O2	112.1(2)
	C11–N12	1.312(7)	N11–C1–N13	119.6(6)	S1–O2	1.458(4)	O1–S1–O3	112.4(3)
	C11–N13	1.328(7)	N12–C1–N13	119.7(6)	S1–O3	1.459(4)	O2–S1–O3	111.3(3)
6	C1–N1	1.318(3)	N1–C1–N2	120.3(2)	S1–O11	1.455(2)	O11–S1–O12	112.1(1)
	C1–N2	1.324(3)	N1–C1–N3	120.3(2)	S1–O12	1.451(2)	O11–S1–O13	112.1(1)
	C1–N3	1.317(3)	N2–C1–N3	119.3(2)	S1–O13	1.454(2)	O12–S1–O13	111.9(1)
7	C1–N1	1.316(6)	N1–C1–N2	119.2(5)	S1–O1	1.452(3)	O1–S1–O2	112.2(2)
	C1–N2	1.329(6)	N1–C1–N3	120.6(5)	S1–O2	1.450(3)	O1–S1–O3	112.9(2)
	C1–N3	1.312(6)	N2–C1–N3	120.1(5)	S1–O3	1.449(3)	O2–S1–O3	112.6(2)
	C11–N11	1.315(6)	N11–C11–N12	120.1(5)	S11–O11	1.446(3)	O11–S11–O12	112.5(2)
	C11–N12	1.306(6)	N11–C11–N13	119.5(5)	S11–O12	1.454(4)	O11–S11–O13	112.4(2)
	C11–N13	1.325(6)	N12–C11–N13	120.4(5)	S11–O13	1.449(3)	O12–S11–O13	112.0(2)
8	C1–N1	1.303(6)	N1–C1–N2	120.2(2)	S1–O1	1.455(3)	O1–S1–O2	111.8(1)
	C1–N2	1.316(4)	N1–C1–N2A	120.2(2)	S1–O2	1.458(2)	O1–S1–O2A	111.8(1)
	C1–N2A	1.316(4)	N2–C1–N2A	119.5(5)	S1–O2A	1.458(2)	O2–S1–O2A	111.1(2)
9	C1A–N1A	1.308(6)	N1A–C1A–N2A	121.0(5)	S1D–O1D	1.455(3)	O1D–S1D–O2D	111.7(2)
	C1A–C2A	1.327(6)	N1A–C1A–N3A	120.3(5)	S1D–O2D	1.460(3)	O1D–S1D–O3D	112.6(2)
	C1A–C3A	1.329(6)	N2A–C1A–N3A	118.7(5)	S1D–O3D	1.460(3)	O2D–S1D–O3D	112.5(2)
	C1C–N1C	1.310(6)	N1C–C1C–N2C	121.7(5)	S1B–O1B	1.451(3)	O1B–S1B–O2B	112.8(2)
	C1C–N2C	1.317(6)	N1C–C1C–N3C	120.1(6)	S1B–O2B	1.460(3)	O1B–S1B–O3B	112.8(2)
	C1C–N3C	1.332(6)	N2C–C1C–N3C	118.1(6)	S1B–O3B	1.455(3)	O2B–S1B–O3B	111.5(2)

atoms in this structure were put in at idealized positions). An θ_{IR} of 157° causes a large distortion in the planarity of the hydrogen-bonded sheets. The single crystal X-ray structure of guanidinium 1-propanesulfonate (**4**) was not solved because suitable crystals could not be grown. However, crystals of **4** have a crystal morphology identical to that of **5**, identical melting points by DSC (153 °C), nearly identical IR spectral peak positions, peak shapes, and peak intensities (Figure 4), and similar densities (d_{exptl} (**4**) $\sim$ 1.18 g/cm^3 and d_{calcd} (**5**) = 1.176). The X-ray powder diffraction patterns for **4** and **5** are similar, although the diffraction peaks exhibited by **4** tend to be less intense and broader, suggesting poorer crystallinity. Notably, comparison of the 2θ value for the intense and broader, suggesting poorer crystallinity. Notably, comparison of the 2θ value for the intense (400) reflections of **4** and **5** reveals that the *a* lattice constant of **4** (13.92 Å) is smaller than that of **5** (14.73 Å), while the difference in the *b* and *c* lattice constants is negligible. This is consistent with the shorter length of the 1-propyl chains, which separate the layers along the *a* direction. These results suggest that **4** is isostructural with **5**.

In guanidinium (1*S*)-(+)-10-camphorsulfonate (**6**), the fully hydrogen-bonded topology is observed. Hydrogen-bonded ribbons along the *a*-axis formed by translationally-related ions connect to screw-related neighboring ribbons by N—H···O hydrogen bonds, with adjacent ribbon planes forming an interribbon dihedral angle, θ_{IR}, of 122°, resulting in an extremely puckered sheet. Hydrogen bonds in this structure have typical geometries, with $d_{N\cdots O}$ lengths varying from 2.90 to 2.96 Å and $\theta_{N—H}$···O angles from 166.0 to 175.7° (note that hydrogen atoms in this structure were put in at idealized positions).

There are two ion pairs per asymmetric unit in guanidinium benzenesulfonate (**7**) and thus 12 unique hydrogen bonds among translationally-related ions. The hydrogen-bonded networks result in sheets parallel to the *ac*-plane. Hydrogen-bonded ribbons run parallel to the *a*-axis, with the ribbons linked to each other along the *c*-axis. Hydrogen bonds vary in $d_{N\cdots O}$ length from 2.89 to 3.06 Å (av 2.94 Å) and $\theta_{N—H\cdots O}$ angle from 150.8 to 178.5° (av 167.4°). The 3.06 Å hydrogen-bond length is the longest of the structures presented here. The ribbons are not coplanar (θ_{IR} = 150°), resulting in puckered hydrogen-bonded sheets. Guanidinium 1-naphthalenesulfonate (**8**) possesses hydrogen-bonded ribbons parallel to the *b*-axis, generated by mirror-related ions. The ribbons are quite planar in **8** ($\theta_{N—H\cdots O}$ = 170.4 and 175.5°) and are nearly orthogonal (θ_{IR} = 77°) to neighboring screw-related ($2_1 \parallel c$) ribbons to which they are hydrogen bonded, resulting in highly puckered hydrogen-bonded sheets. The interribbon hydrogen bond is longer ($d_{N\cdots O}$ = 2.98 Å) than the intraribbon hydrogen bonds ($d_{N\cdots O}$ = 2.86 and 2.94 Å). Within the hydrogen-bonded ribbon, **8** contains the shortest N—H···O length of the structures presented, 2.86 Å (a hydrogen bond of this length also occurs in **5**). In contrast, guanidinium 2-naphthalenesulfonate (**9**) possesses nearly planar hydrogen-bonded sheets, with 12 hydrogen bonds per asymmetric unit between translationally-related ions parallel to the *ac*-plane. These hydrogen bonds vary in $d_{N\cdots O}$ length from 2.86 to 3.02 Å (av 2.94 Å) and in $\theta_{N\text{-}H\cdots O}$ angle from 152.3 to 177.6° (av 167.2°), with an θ_{IR} of 146°. These structural features resemble those of the isostructural salt **7**.

Layering in Guanidinium Sulfonates. After self-assembly of guanidinium and sulfonate ions into two-dimensional sheets **III**, further self-assembly occurs into one of two different motifs (Chart 2). One of these motifs (*bilayer*) is described by repeating bilayers in which the sulfonate R groups of each sheet are oriented on the same side, with interpenetrating R groups within the bilayer directed toward each other and Coulombic interactions between opposing hydrogen-bonded sheets. The other motif (*single layer*) has sheets in which the sulfonate R groups within a ribbon are located on one side of the ribbon but alternate sides from ribbon to ribbon. In Chart 2, neighboring ribbons are shaded differently for clarity. Both packing patterns result in partitioning into hydrophobic regions containing the organic sulfonate R groups and polar regions containing the guanidinium sulfonate hydrogen-

Table 3. Hydrogen-Bond Geometries of 1–3 and 5–9

compound	intraribbon (dimer A + dimer B): symmetry of dimer A ions	dimer A[a]: $d_{N\cdots O}$ (Å)	dimer A[a]: $\theta_{N-H\cdots O}$ (deg)	symmetry relating dimer A and dimer B ions	dimer B[a]: $d_{N\cdots O}$ (Å)	dimer B[a]: $\theta_{N-H\cdots O}$ (deg)	interribbon (dimer C linkage): symmetry of dimer C	dimer C[a]: $d_{N\cdots O}$ (Å)	dimer C[a]: $\theta_{N-H\cdots O}$ (deg)	interribbon dihedral angle, θ_{IR} (deg)
1	asymmetric unit			*m* ⊥ *b*			*c*-centering, *m* ⊥ *b*			
	N1—H1···O2	2.917(3)	168.19	N1—H1A···O2A	2.917(3)	168.19	N2—H3···O2	2.935(3)	158.26	171
	N2—H2···O1	2.893(2)	160.60	N2A—H2A···O1A	2.893(2)	160.60	N2A—H3A···O2A	2.935(3)	158.26	
2	*C*-centering			*C*-centering, translation along *y*			asymmetric unit			
	N2—H4···O2	2.998(3)	170.12	N1—H2···O1	2.986(3)	175.37	N1—H1···O2	2.990(4)	175.48	163
	N3—H5···O1	3.001(3)	177.23	N2—H3···O3	2.992(3)	174.02	N3—H6···O3	2.985(4)	173.47	
3	asymmetric unit			*m* ⊥ *b*			*C*-centering, *m* ⊥ *b*			
	N2—H3···O1	2.927(3)	178.19	N2A—H3A···O1A	2.927(3)	178.19	N1—H2···O1	2.957(3)	159.62	170
	N1—H1···O2	2.957(4)	167.91	N1A—H1A···O2A	2.957(4)	167.91	N1A—H2A···O1A	2.957(3)	159.62	
5	asymmetric unit			*c* ⊥ *b*, translation along *y*,*z*			2_1 ∥ *c*, translation along *x*,*z*			
	N13—H15···O1	2.958(6)	174.04	N12—H12···O3	2.904(7)	155.23	N13—H14···O3	2.903(6)	165.90	157
	N12—H13···O2	2.860(6)	157.37	N11—H10···O2	2.995(6)	153.68	N11—H11···O1	2.916(6)	172.94	
6	asymmetric unit			translation along *x*			2_1 ∥ *c*, translation along *x*,*z*			
	N1—H1···O11	2.897(3)	174.07	N1—H2···O13	2.902(3)	173.19	N2—H4···O13	2.912(3)	175.72	122
	N3—H6···O12	2.941(3)	169.92	N2—H3···O12	2.960(3)	166.08	N3—H5···O11	2.933(3)	175.37	
7	asymmetric unit			translation along *x*			asymmetric unit			
	N1—H2···O1	2.885(6)	175.82	N2—H4···O2	3.060(7)	157.36	N11—H21···O3	2.888(6)	176.56	150
	N2—H3···O3	2.997(7)	162.01	N3—H5···O1	2.900(7)	173.52	N13—H26···O2	2.905(6)	178.49	
	asymmetric unit			translation along *x*			translation along *z*			
	N11—H22···O11	2.979(7)	167.56	N12—H24···O12	2.891(7)	173.80	N1—H1···O13	2.928(6)	156.52	
	N12—H23···O13	2.896(7)	170.96	N13—H25···O11	2.973(7)	164.98	N3—H6···O12	2.944(5)	150.83	
8	asymmetric unit			*m* ⊥ *b*			2_1 ∥ *c*			
	N1—H1A···O2	2.861(3)	170.44	N1A—H1···O2A	2.861(3)	170.44	N2—H3···O2	2.979(4)	167.09	77
	N2—H2···O1	2.938(4)	175.48	N2A—H2A···O1A	2.938(4)	175.48	N2A—H3A···O2A	2.979(4)	167.09	
9	translation along *x*,*z*			translation along *z*			asymmetric unit			
	N3A—H13···O1D	2.893(6)	174.44	N2A—H11···O3D	3.017(6)	169.11	N1A—H8···O2B	2.913(6)	177.52	146
	N1A—H9···O3D	2.963(6)	168.63	N3A—H12···O2D	2.883(6)	165.80	N2A—H10···O1B	2.896(5)	177.64	
	asymmetric unit			translation along *x*			asymmetric unit			
	N1C—H22···O3B	2.863(6)	170.02	N2C—H24···O3B	2.887(6)	160.99	N1C═H21···O2D	2.956(6)	160.33	
	N3C—H26···O1B	3.017(7)	165.41	N3C—H25···O2B	2.983(7)	163.70	N2C—H23···O1D	3.009(6)	152.31	

[a] See structures III in Chart 1 for dimer A, B, and C definitions.

Chart 1

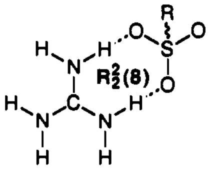

I

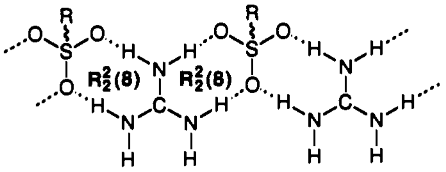

II

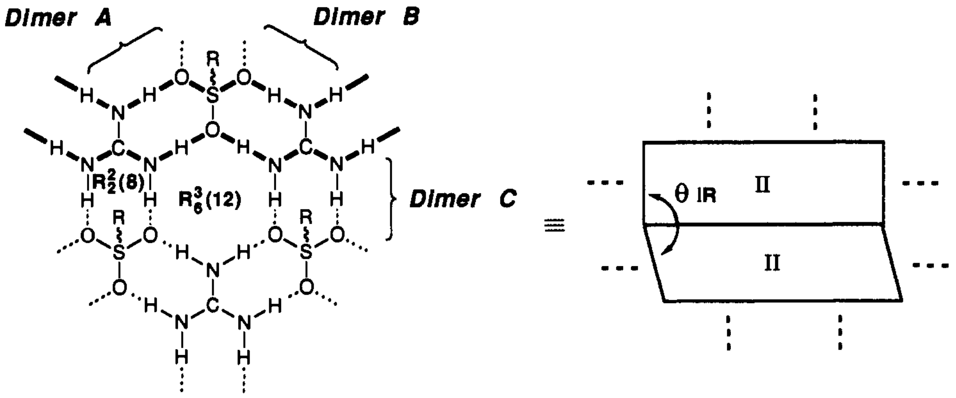

III

bonding network. In all cases, R groups of adjacent layers interpenetrate to maximize favorable van der Waals contacts. Often the sheets are puckered to accommodate closer packing of the R groups. The layering in guanidinium sulfonates can be

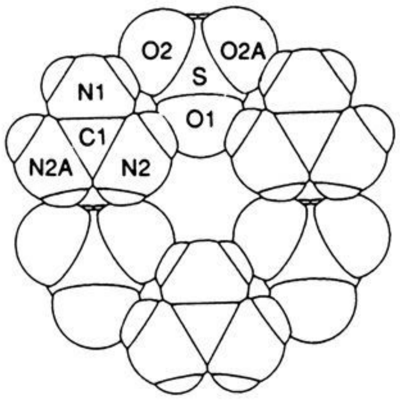

Figure 2. Space-filling view normal to guanidinium ion in **1** showing the quasihexagonal hydrogen-bonded sheet.

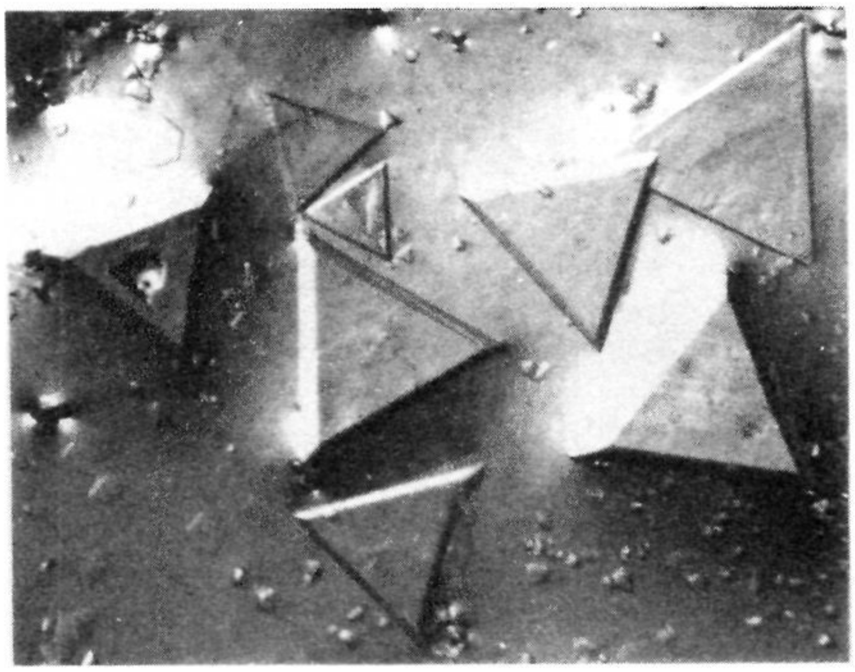

Figure 3. Photograph of crystals of **1**, scale about 1 mm per side of larger triangular crystals.

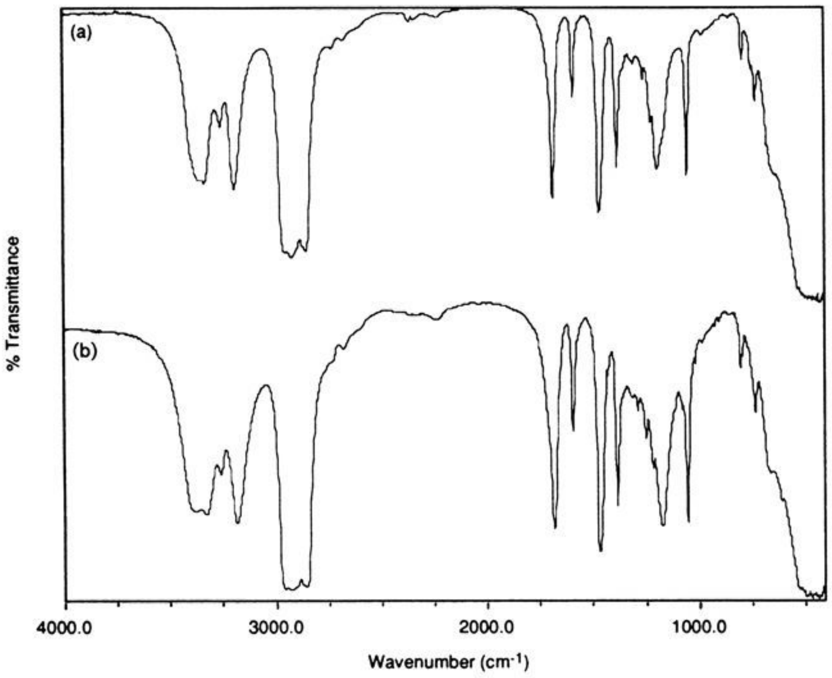

Figure 4. Comparison of the IR spectra of (a) guanidinium 1-propanesulfonate (**4**) and (b) guanidinium 1-butanesulfonate (**5**).

described by the spacings in the polar and hydrophobic regions for bilayer salts and the spacing between hydrogen-bonded layers in single layer salts. These spacings are referred to as d_I (ionic spacing), d_{VDW} (van der Waals spacing), and d_{SL} (spacing in single layer salts). The dihedral angle between ribbon planes, θ_{IR} (interribbon dihedral angle), is also shown in the Chart 2 (see also structure **III** in Chart 1 and Table 3).

Guanidinium Sulfonates with Bilayer Structures. Guanidinium salts of methanesulfonate (**1**), triflate (**2**), ethanesulfonate (**3**), benzenesulfonate (**7**), and 2-naphthalenesulfonate (**9**) crystallize with bilayer structures in monoclinic space groups. Each structure is composed of two-dimensional guanidinium sulfonate hydrogen-bonded sheets, as in **III**. These sheets are parallel to the *ab* plane in structures **1**, **2**, and **3** and to the *ac* plane in **7** and **9**. Stereoviews showing the bilayer structures of these salts are given in Figure 5.

Chart 2

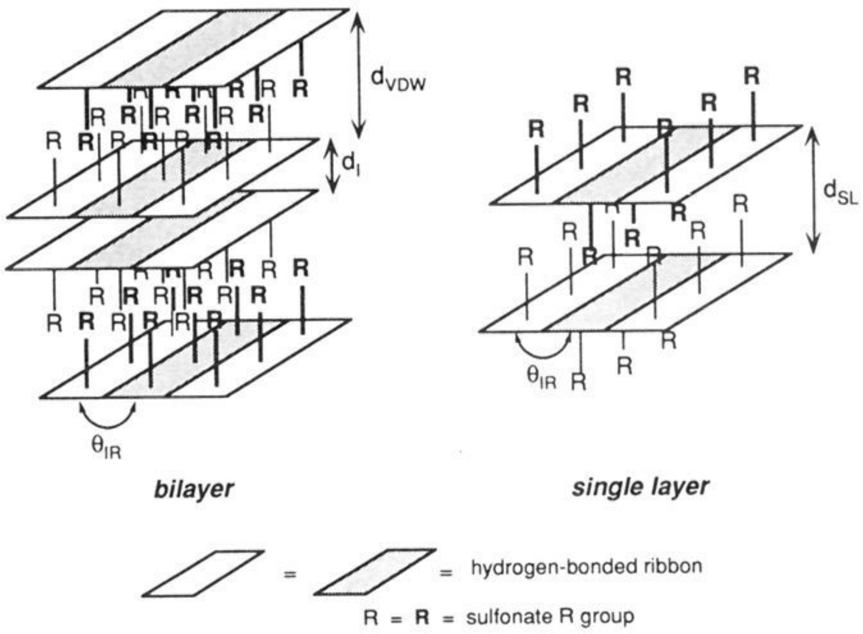

Guanidinium ethanesulfonate (**3**) is isostructural with **1**. The cell parameters *a*, *b*, and *β* for both salts are nearly identical; however, the *c* lattice constant of **3** (the direction approximately normal to the hydrogen-bonded sheet) is considerably longer (11.172 versus 9.998 Å for **1**) in order to accommodate packing of the additional methylene unit. Guanidinium triflate (**2**) has a similar structure; however, it crystallizes in space group $C2/c$. The slight difference is probably due to electronic differences between $-CH_3$ and $-CF_3$ groups. Guanidinium benzenesulfonate (**7**) also crystallizes with a bilayer structure, in space group $P2_1/c$, but with distortion of the hydrogen-bonded sheets to allow for efficient packing of the larger phenyl groups. Guanidinium 2-naphthalenesulfonate (**9**) is isostructural with **7**. The *a* and *c* unit cell lengths, corresponding to the two dimensions of the hydrogen-bonded sheets, are almost identical, $a = 7.50(1)$ and 7.495(6) and $c = 12.060(2)$ and 12.040(3) Å, and *β* angles similar, 92.24(8) and 91.29(5)°, for **7** and **9**, respectively. However, the *b* lattice constant of **9** (28.35 Å) is greater than that of **7** (23.29 Å) because of the larger naphthyl groups between hydrogen-bonded layers. The interlayer aryl ring interactions in **7** and **9** result in a herringbone motif (Figure 6a and b). In bilayer salts the two-dimensional hydrogen-bonded networks are rather planar but distort more in order to accommodate larger R groups, as evidenced by the interribbon dihedral angles, θ_{IR}, which range from 171° for small R (methyl) to 146° for larger R (2-naphthyl).

Electrostatic interactions play a role in the crystal packing of bilayer salts; positively-charged guanidinium cations are situated in proximity to negatively-charged sulfonate anions in adjacent sheets. In all cases, an eclipsed orientation of guanidinium ions with respect to sulfonate ions of neighboring layers is observed. The Coulombic interactions can be characterized by considering each hydrogen-bonded layer as a hexagonal net of alternating positive and negative charges (Scheme 1). The relationship between oppositely-charged ions in adjacent layers is determined by the (d_m,d_n) offset.[23] Ideal alignment of opposing layers, based solely on Coulombic factors, would be that in which oppositely charged ions are located directly across from one another, with a (d_m,d_n) offset of (0, 0). The offsets for each bilayer structure are given in Table 4. In most cases, the n-offset is nearly zero, with a measurable offset occurring mainly along one direction, along the C–N and S–O bond directions (m-direction in Scheme 1). The exception occurs in **2**, in which the offset is approximately perpendicular to the C–N and S–O m-direction.

---

[23] The (d_m,d_n) offset is taken as the average offset of each guanidinium nitrogen atom of the asymmetric unit with its nearest symmetry-related sulfonate oxygen atom in the adjacent layer across the ionic region. For **1**, **2**, and **3**, the (d_m,d_n) offset corresponds to offsets in the (x, y) planes. For **7** and **9**, the offset corresponds to offsets in the (z, x) planes.

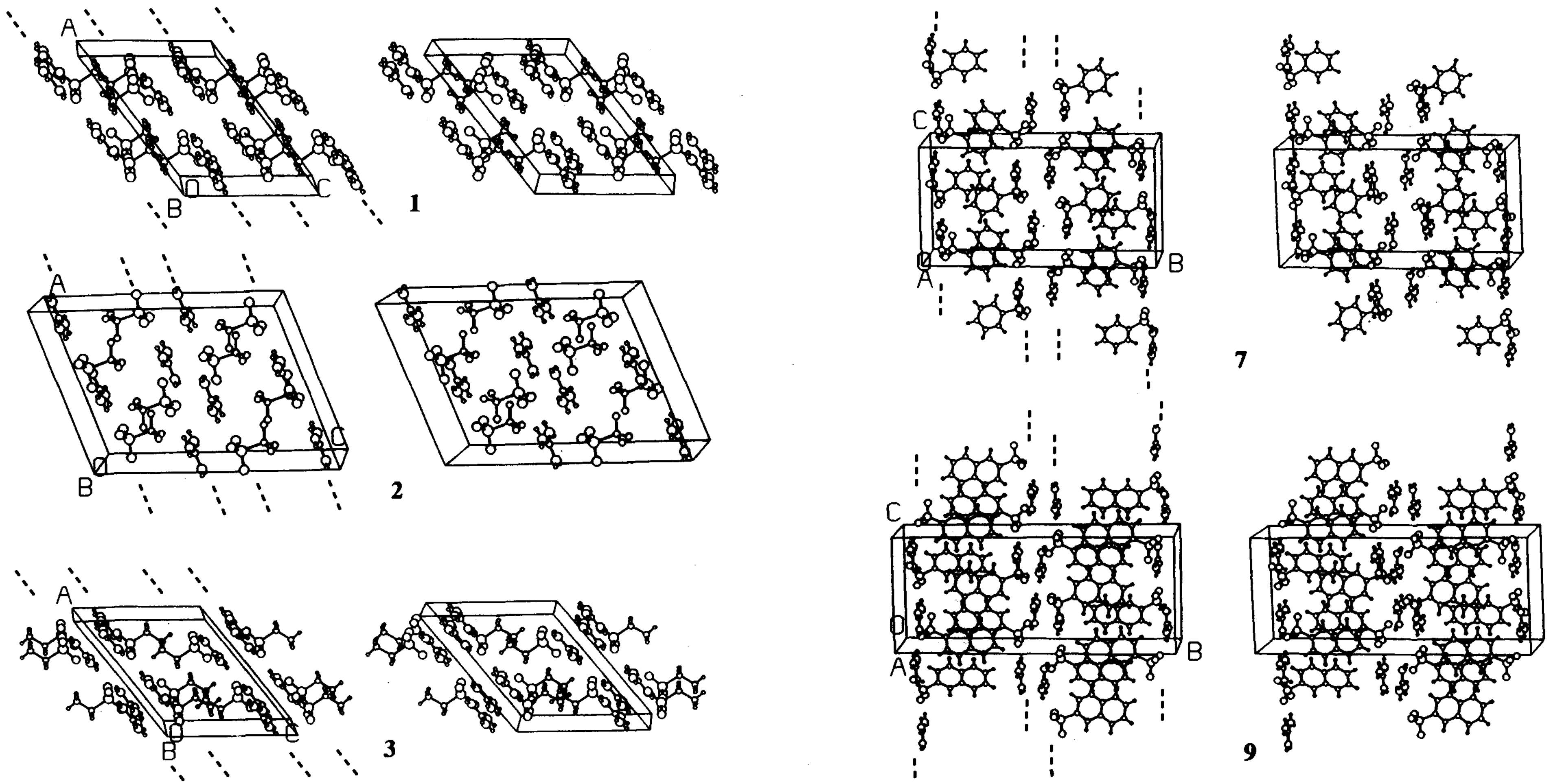

Figure 5. Stereoviews approximately along hydrogen-bonded layers in bilayer salts. The dashed lines indicate the mean planes containing the hydrogen-bonded sheets. Note that the hydrogen-bonded *ribbons* contained in the sheet project normal to the plane of the paper.

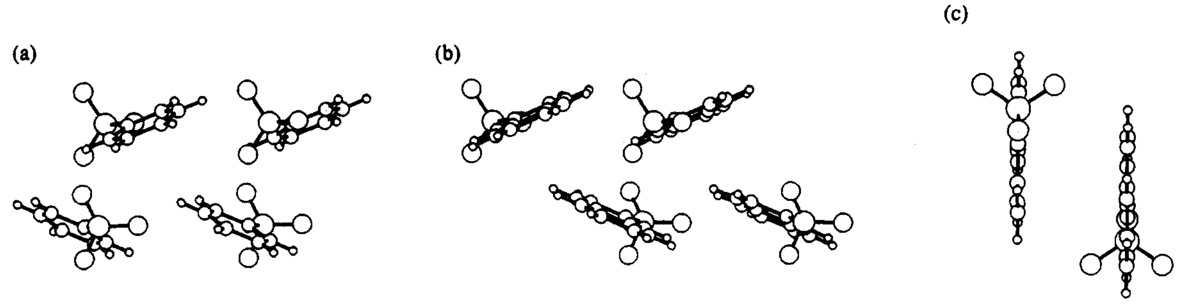

Figure 6. Interlayer aryl ring interactions, viewed along the *b*-axes in isostructural bilayer salts (a) **7** and (b) **9** and along the along the *a*-axis in single layer salt (c) **8**. Guanidinium ions have been omitted for clarity.

Scheme 1

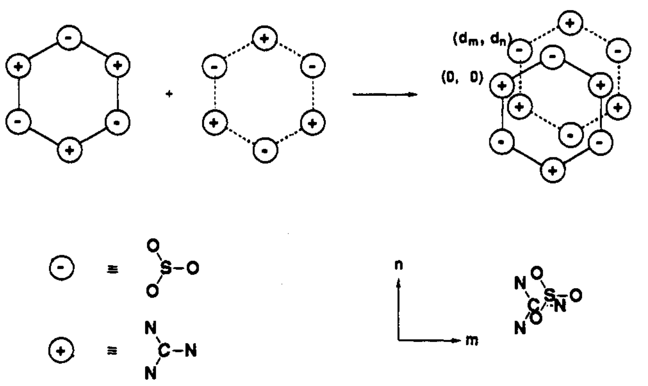

Interlayer interactions in bilayer salts are described by Coulombic interactions in the polar region between opposing hydrogen-bonded sheets and van der Waals interactions between R groups of adjacent layers in the hydrophobic region (see Chart 2, bilayer). The ionic spacing between hydrogen-bonded sheets, d_I,[24] is roughly identical for all the bilayer structures, averaging 3.64 Å (see Table 4). The spacing of the hydrophobic region where R groups interpenetrate, d_{VDW},[27] increases with increasing size of R. Note that the offset and interlayer spacings given in Table 4 are determined from mean planes, and nonplanarity resulting from twisting of atoms out of the hydrogen-bonded plane results in locally different interplanar spacings.

Guanidinium Sulfonates with Single Layer Structures. Guanidinium 1-butanesulfonate (**5**), guanidinium (1*S*)-(+)-10-camphorsulfonate (**6**), and guanidinium 1-naphthalenesulfonate (**8**) crystallize with distorted single layer structures (Figure 7) in orthorhombic and monoclinic crystal systems. In these salts, the hydrogen-bonded sheets are highly puckered because the hydrogen-bonded ribbons twist out of the sheet plane. Interestingly, in **5** (space group *Pbcn*) the ions pack with a lower density than that typically found in guanidinium sulfonates (1.176 compared with 1.35–1.40 g/cm³). The alkyl chains (using the vector S1–C(1-butylposition)) are tilted approximately 65° relative to the sulfonate O1–O2–O3 plane, with van der Waals interactions between butyl chains. Salts **6** and **8** crystallize with similar single layer structures in which the ribbons have a zigzag motif when viewed along *a*- and *b*-axes, respectively. This motif is a consequence of nearly planar hydrogen-bonded ribbons linked by hydrogen bonding to neighboring ribbons with a nearly orthogonal θ_{IR}. In **6** (space group $P2_1$) the chiral camphor group packs with pseudoinversion centers between the hydrogen-bonded layers. In **8** (space group *Pnma*) face-to-face stacking (see Figure 6c) of naphthyl rings (interplanar distance ≈ 4.1 Å) occurs in hydrophobic regions between hydrogen-bonded layers.

Ionic interactions in these salts are more difficult to ascertain. The distances between sheets are not clearly defined but can be taken as the distance d_{SL}[25] between planes defined by guanidinium carbon atoms within a single layer (see Chart 2, single layer). These distances are equivalent to one-half of the *a*-constant (7.37 Å), the *c*-constant (9.30 Å), and one-half of the *a*-constant (10.71 Å) for **5**, **6**, and **8**, respectively.

Discussion

Solid-state molecular packing of guanidinium sulfonates is a consequence of hydrogen-bonding, ionic, and van der Waals interactions. The guanidinium sulfonate salts crystallize with two-dimensional hydrogen-bonded networks (**III**, Chart 1) in which the planar guanidinium cation forms six hydrogen bonds to oxygen lone electron pairs on each of three neighboring sulfonate anions. This solid-state packing motif is important because packing is effectively controlled in two dimensions through hydrogen-bond interactions, an advantage in crystal engineering. The recurrence of the two-dimensional hydrogen-bond motif probably results from a combination of stabilizing factors: the large number of hydrogen bonds, matched number of donors and acceptors, three-fold topologies for both the guanidinium and RSO_3^- ions, and Coulombic interactions between oppositely charged ions. An important feature of the guanidinium sulfonate system is the potential for engineering the 3-D structure by appropriate choice of sulfonate organic group. Packing in the third dimension is determined by steric constraints and van der Waals interactions of the sulfonate R groups, as well as Coulombic interactions between oppositely charged ions in adjacent layers. The preservation of the hydrogen-bonded sheet motif in these structures is favored by the absence of hydrogen-bonding sites on the sulfonate R groups that would otherwise compete for hydrogen-bonding sites on the guanidinium or sulfonate ions. However, if the steric requirements of the R groups are severe, the planarity of the hydrogen-bonded sheet motif is disrupted.

The two-dimensional hydrogen-bonded sheet motif **III** has not been reported previously. A search of the Cambridge Structural Database[26] produced no structures of guanidinium sulfonate salts but did produce structures of several compounds containing the 1,2-protonated guanidyl N–C(NH)NH and sulfonate SO_3 functionalities. Dimers **I** and ribbons **II** (Chart 1) occur in several of these compounds, both in guanidyl sulfonate salts (dimers,[27]

---

(24) The ionic spacing, d_I, is calculated as [(average coordinate of the guanidinium nitrogen atoms and sulfonate oxygen atoms of the asymmetric unit) – (average coordinate of the guanidinium nitrogen atoms and sulfonate oxygen atoms of the symmetry-related ion pair(s))] of the coordinate corresponding to the direction approximately perpendicular to the hydrogen-bonded layer. For **1**, **2**, and **3**, this is the *z*-coordinate, and for **7** and **9**, the *y*-coordinate. The van der Waals spacing, d_{VDW}, is calculated as [(appropriate cell constant (or fraction of cell constant)) – d_I]. The appropriate fractions of cell constants for **1** and **3** are the *c*-constants, for **2**, one-half of the *c*-constant, and for **7** and **9**, one-half of the *b*-constant.

(25) The distance between hydrogen-bonded single layers, d_{SL}, is taken to be the distance between the center of guanidinium ions in neighboring layers. This is one-half of the *a*-constant for **5** and **8**. For **6**, the *c*-constant represents the interlayer spacing distance.

(26) *Cambridge Structural Database*; Cambridge Crystallographic Data Centre, University Chemical Library: Cambridge, England, update April, 1993; Version 5.05.

(27) (a) Doubell, P. C. J.; Oliver, D. W.; Van Rooyen, P. H. *Acta Crystallogr.* **1991**, *C47*, 353. (b) Griffin, R. J.; Meek, M. A.; Schwalbe, C. H.; Stevens, M. F. G. *J. Med. Chem.* **1989**, *32*, 2468. (c) Sutton, P. A.; Cody, V. *J. Crystallogr. Spectrosc. Res.* **1988**, *18*, 755. (d) Cody, V. *Acta Crystallogr.* **1984**, *C40*, 1000. (e) Cody, V.; Zakrzewski, S. F. *J. Med. Chem.* **1982**, *25*, 427.

Table 4. Ionic Net Offsets and Interlayer Spacings between Layers in Bilayer Structures (See Scheme 1 and Ref 23 for Offset Definitions and Chart 3 and Ref 24 for d_I and d_{VDW} Definitions.)

compd	coordinates of symmetry-related ion pair(s)[a]	ionic net offset			interlayer spacing	
		coordinates used[b]	(d_m, d_n) (Å)	coordinate used[c]	d_I (Å)	d_{VDW} (Å)
1	$^3/_2 - x, ^1/_2 - y, 1 - z$	(x, y)	(0.77, 0.02)	z	4.04	5.96
2	$^1/_2 - x, ^1/_2 - y, -z$	(x, y)	(0.27, 1.50)	z	3.40	5.71
3	$^3/_2 - x, ^1/_2 - y, 1 - z$	(x, y)	(0.86, 0.04)	z	4.06	7.11
7[d]	$1 - x, -y, 1 - z$ $2 - x, -y, 1 - z$	(z, x)	(2.06, 0.06)	y	3.33	8.31
9[d]	$-x, -y, 2 - z$ $1 - x, -y, 1 - z$	(z, x)	(2.02, 0.04)	y	3.35	10.82

[a] Guanidinium nitrogen atoms of the asymmetric unit and sulfonate oxygen atoms of the nearest symmetry-related anion in the opposing layer were used in the offset and spacing calculations. [b] The coordinates used are the unit cell directions corresponding to (d_m, d_n) directions. [c] The coordinate used is the unit cell direction corresponding to the d_I/d_{VDW} direction. [d] For **7** and **9**, the asymmetric unit contains two guanidinium ions which were nearest to sulfonate oxygens of two different (but translationally-related) ion pairs. The calculations are an average of the relationships involving both guanidinium ions of the asymmetric unit and the two symmetry-related ion pairs.

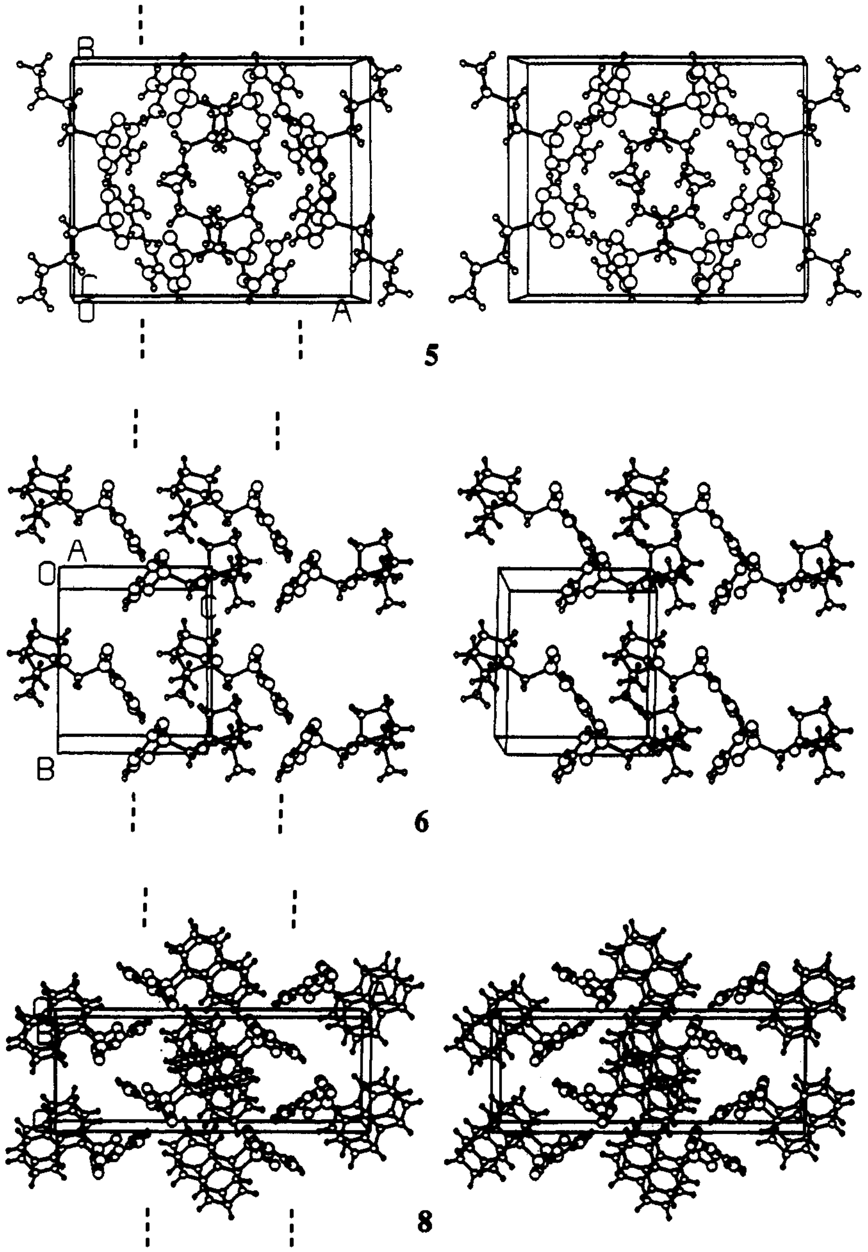

Figure 7. Stereoviews approximately along hydrogen-bonded layers in single layer salts. The dashed lines indicate the mean planes containing the hydrogen-bonded sheets. Note that the hydrogen-bonded *ribbons* contained in the sheet project normal to the plane of the paper.

ribbons[28]) and in molecules in which guanido and sulfonate functionalities are attached to the same molecule, forming dimers[29] or ribbons[30] (for examples, see Chart 3). The hydrogen-bond lengths and angles in these compounds compare favorably with those we have found in guanidinium sulfonates. The structural features of the hydrogen bonds in guanidinium sulfonates (Table 3) are similar to those found in these related structures, although

---

(28) (a) McCourt, M.; Cody, V. *J. Am. Chem. Soc.* **1991**, *113*, 6634. (b) Matsumoto, O.; Taga, T.; Machida, K. *Acta Crystallogr.* **1989**, *C45*, 913. (c) Nakamura, H.; Iitaka, Y. *Acta Crystallogr.* **1978**, *B34*, 3384.

Chart 3

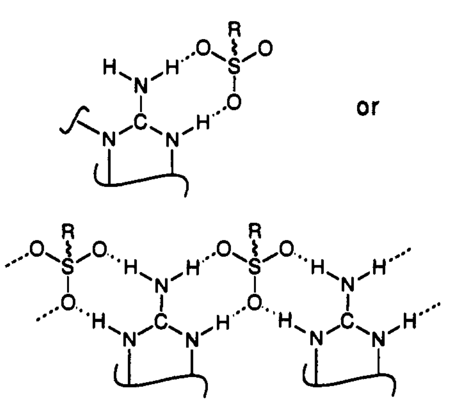

the bond lengths in our salts are generally longer. This behavior can be attributed to the greater number of hydrogen bonds per guanidinium ion in the salts described here, so that no one hydrogen bond (or pair of hydrogen bonds) dominates.

Hydrogen-bonded dimers, ribbons, or sheets in guanidinium sulfonates are not consistently planar, for example, the two hydrogen bonds that form a dimer do not have the same hydrogen-bond lengths or angles. Presumably the deviation is due to solid-state packing of the sulfonate R groups. Dimers range from very planar to very skewed. The largest variation in hydrogen bonding within a dimer occurs in **9**, which has one short hydrogen bond ($d_{N\cdots O}$ = 2.863(6) Å) and one long (3.017(7) Å) and $\theta_{N-H\cdots O}$ angles of 170.02 and 165.41°. The variety of hydrogen-bond lengths and angles found in guanidinium sulfonates, a reflection of hydrogen-bond strength, explains the range and number of bands in the N-H stretching and bending and the S-O stretching regions of the IR spectra.

Ionic interactions play a large role in the solid-state structures. Bilayers are held together by Coulombic forces, with guanidinium ions often in proximity to sulfonate groups of neighboring layers. In all cases each positively-charged guanidinium ion is surrounded by three negatively-charged sulfonate ions as a consequence of hydrogen bonding and interacts with another sulfonate of a neighboring layer. Van der Waals contacts are also important interlayer interactions, with distortion of hydrogen-bonded sheets from planarity frequently occurring in order to maximize R-R contacts. Partitioning of the guanidinium sulfonate sheets into layered hydrophobic and polar regions is similar to behavior observed in many other organic compounds, for example, in amino acids and small acyclic peptides[31] and carboxylic acids containing long alkyl chains.[32] Indeed, the guanidinium sulfonate compounds bear striking resemblance to other classes of layered solids, particularly metal phosphonates.[33] These materials have been shown to possess two-dimensional layers of strong metal-oxide bonds, such as Zr-O(phosphonate), separated by regions containing organic R groups of the phosphonate. Guanidinium sulfonates are similar to these materials in that the layer assembled by guanidinium sulfonate N—H···O hydrogen bonds has strong two-dimensional bonding, and the sulfonate residue provides for hydrophobic regions that separate the layers (Figure 8). However, the hydrophobic R group regions in guanidinium sulfonates interpenetrate to maximize van der Waals interactions, whereas in zirconium phosphonates this is not the case.

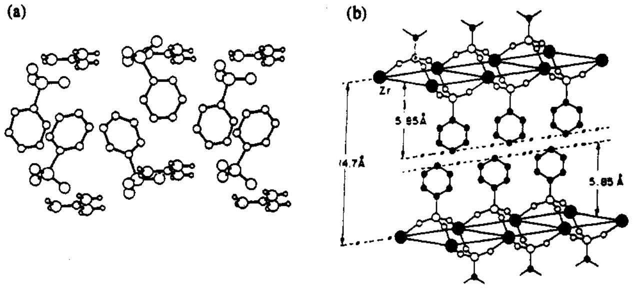

Figure 8. Comparison of guanidinium sulfonate to zirconium phosphonate layered structures: (a) molecular packing of a (010) bilayer in guanidinium benzenesulfonate (**7**) (from this work) and (b) schematic representation of a bilayer in zirconium phenylphosphonate (reproduced from ref 33c with permission).

Scheme 2

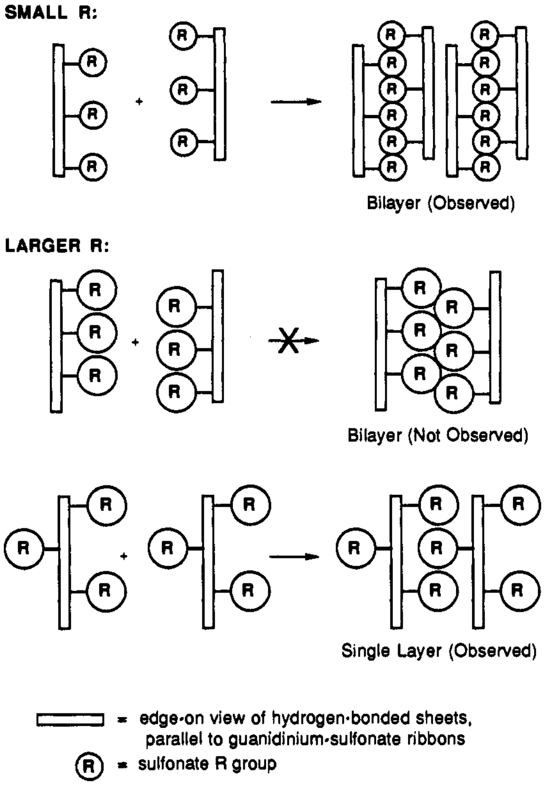

While two-dimensional structure in guanidinium sulfonates is controlled by hydrogen-bonding interactions, assembly in the third dimension is influenced by choice of sulfonate organic group R. Factors determining packing into bilayer or single layer structures include steric constraints for bulky R groups (Scheme 2) as well as favorable interlayer interactions, such as van der Waals and aryl π-stacking interactions. Assuming symmetrical bond lengths of C-N 1.32 Å and S-O 1.45 Å, a planar array, tetrahedral sulfur atom, and the sum of van der Waals radii of N···O as the maximum hydrogen-bond distance (3.07 Å[20]), the distance between the centers of guanidinium and sulfonate groups in a hydrogen-bonded sheet is approximately 4.75 Å. Bilayer structures are favored for small R groups, as the low density of hydrocarbon content on the hydrogen-bonded sheet allows interdigitation of layers (Scheme 2, see also Chart 2, bilayer). This provides for favorable Coulombic interactions between layers *and* van der Waals interactions between R groups. It is also feasible that hydrogen-bonded sheets will distort from planarity to relieve steric crowding or to accommodate closer packing of the R groups. In salts with larger R groups (i.e., groups wider than the ion center-to-center distance of 4.75 Å), orientation of all the R groups to the same side of each hydrogen-bonded sheet

---

(29) (a) Destro, R.; Maghini, A.; Merati, F. *Acta Crystallogr.* **1987**, *C43*, 949. (b) Kim, Y. B.; Wakahara, A.; Fujiwara, T.; Tomita, K.-I. *Bull. Chem. Soc. Jpn.* **1973**, *46*, 2194. (c) Pitman, I. H.; Shefter, E.; Ziser, M. *J. Am. Chem. Soc.* **1970**, *92*, 3413.

(30) Bombieri, G.; Demartin, F.; Braghiroli, D.; Di Bella, M. *J. Crystallogr. Spectrosc. Res.* **1990**, *20*, 403.

(31) Gorbitz, C. H.; Etter, M. C. *Int. J. Pept. Protein Res.* **1992**, *39*, 93.

(32) (a) Bryan, R. F.; Hartley, P. *Mol. Cryst. Liq. Cryst.* **1980**, *62*, 259. (b) Bryan, R. F.; Hartley, P.; Miller, R. W.; Shen, M.-S. *Mol. Cryst. Liq. Cryst.* **1980**, *62*, 281.

(33) For reviews, see: (a) Clearfield, A. *Comments Inorg. Chem.* **1990**, *10*, 89. (b) Alberti, G. In *Recent Developments in Ion Exchange*; Williams, P. A., Hudson, M. J., Eds.; Elsevier Applied Science: New York, 1987; p 233. (c) Alberti, G.; Costantino, U.; Allulli, S.; Tomassini, N. *J. Inorg. Nucl. Chem.* **1978**, *40*, 1113.

is still allowed on the basis of steric considerations. However, under these conditions, the R groups residing on a hydrogen-bonded sheet would tend to be rather closely packed, reducing van der Waals contacts between the R groups of two approaching sheets. That is, interpenetration of R groups from the different sheets would not be possible without *severe* disruption of the hydrogen-bond motif. In these cases, hydrogen-bonded sheets composed of ribbons in which R groups within a ribbon are oriented to the same side of the ribbon but which alternate orientation from ribbon to ribbon (see Chart 2, single layer) are observed. This arrangement allows for interdigitation of R groups in hydrophobic regions, maximizing favorable R–R van der Waals contacts (Scheme 2). The linkage of ribbons in bilayer and single layer structures also differs. In bilayer structures ribbons link approximately coplanar (θ_{IR} approaching 180°), whereas in single layer structures ribbon planes are nearly orthogonal, causing distortion of the hydrogen-bonded sheets from planarity. The observed structures therefore reflect a balance between hydrogen-bonding forces associated with the guanidinium sulfonate sheet and van der Waals forces between sulfonate R groups.

The preference for bilayer versus single layer motifs can be illustrated by comparison of the guanidinium *n*-alkanesulfonate series, guanidinium 1- and 2-naphthalenesulfonates, and guanidinium (1*S*)-(+)-10-camphorsulfonate. The guanidinium *n*-alkanesulfonate series evolves from bilayer to single layer structures with increasing R chain length. As the alkyl group increases in length, its conformational freedom increases, and the chain can be oriented in many directions relative to the C–S bond. Guanidinium salts of sulfonates with small alkyl groups such as methyl (**1**), trifluoromethyl (**2**), and ethyl (**3**), pack in bilayer structures in monoclinic space groups. Although the single crystal X-ray structure of the 1-propyl salt **4** has not been solved (it crystallizes as fibrous needles unsuitable for X-ray analysis), the experimental data (nearly identical solid-state IR spectra, melting points, densities, and crystal morphologies) suggest that **4** is isostructural with **5**, which has a single layer-type structure. Furthermore, the *a* lattice constant of **4** is smaller than that of **5**, consistent with the shorter length of the 1-propyl chains which separate the layers along the *a* direction. Although the size/width constraint should not affect packing of the butyl chain and bilayer packing would be expected, single layer packing of "wavy" hydrogen-bonded sheets appears to allow for more efficient packing of the flexible chains.

The position of attachment of the sulfonate group to the naphthyl moiety also causes variation in the solid-state layered structure. Guanidinium 1-naphthalenesulfonate (**8**) crystallizes with a single layer structure, whereas the 2-naphthyl salt **9** has a bilayer structure. The naphthyl moiety is rigid and planar and thus has limited conformational mobility. The width of the naphthalene ring in **8**, 4.83 Å, is longer than the calculated distance between ion centers (4.75 Å), which dictates the available space for bilayer packing. The orientation of the naphthyl groups in **8** prevents interdigitation of naphthyl groups in a bilayer structure. Instead of interdigitation accompanied by disruption of hydrogen-bonded sheets, the naphthyl groups of adjacent ribbons orient to opposite sides of the hydrogen-bonded layer, assembling into a single layer structure. The hydrogen-bonded sheets remain intact but subsequently distort to allow for face-to-face stacking of naphthyl rings of neighboring layers. In **9**, the naphthyl group is oriented more nearly along the three-fold axis of the -SO$_3$ group, thus decreasing its effective width. This results in a less densely packed arrangement of the naphthyl groups when they are all oriented on the same side of the hydrogen-bonded sheets, favoring subsequent interdigitation of naphthyl groups from approaching sheets into a bilayer structure. The interlayer interactions in **8** are π-stacking, commonly found in organic crystal structures, while those in **9** are herringbone edge-to-face interactions involving the naphthyl rings (see Figure 6a and c), commonly found in the crystal structures of benzene, naphthalene, and aromatics[34] with small C–H ratios. Although compounds **8** and **9** pack with different solid-state structures, they have identical calculated densities of 1.39 g/cm^3, indicating close packing in both compounds.

Conclusions

The single crystal X-ray structures of guanidinium alkane- and arenesulfonates clearly indicate that crystal packing is strongly directed by formation of two-dimensional hydrogen-bonded sheets. The motif is preserved for a diverse variety of sulfonate R groups, ranging from linear alkanesulfonates to bulky arene- and camphorsulfonates. The degree of distortion of hydrogen-bonded sheets and the preference for bilayer and single layer structures are dictated by the size of the sulfonate R group. The strong tendency of the guanidinium alkane- and arenesulfonates to form two-dimensional sheets coupled with the ability to alter the R groups without disruption of the sheet topology represents a viable approach to molecular-level engineering of new materials. For example, the chiral R group in **6** results in crystallization into a noncentrosymmetric space group and trace SHG activity. It is reasonable to suggest that, even when chiral R groups are absent, hydrogen-bonding and Coulombic interactions may override dipolar interactions which often bias molecules to pack in centrosymmetric arrangements (canceling all nonlinear optical activity).[35] Indeed, studies currently in progress in our lab support this contention.[36] We also anticipate that the low dimensionality of this class of molecular solids will lead to materials with novel conductivity and magnetic properties.

Acknowledgment. We gratefully acknowledge Professor Doyle Britton and Elise Sudbeck, Department of Chemistry, University of Minnesota, for crystallographic assistance and the Office of Naval Research (N0014-89-K-1301) for financial support.

Supplementary Material Available: Positional parameters, anisotropic thermal parameters, intra- and intermolecular bond lengths and angles, and unit cell drawings for eight crystal structures (172 pages); tables of observed and calculated structure factors (116 pages). This material is contained in many libraries on microfiche, immediately follows this article in the microfilm version of the journal, and can be ordered from the ACS; see any current masthead page for ordering information.

---

(34) (a) Perutz, M. F.; Fermi, G.; Abraham, D. J.; Poyart, C.; Bursaux, E. *J. Am. Chem. Soc.* **1986**, *108*, 1064. (b) Pawliszyn, J.; Szczesniak, M. M.; Schiener, S. *J. Phys. Chem.* **1984**, *88*, 1726.

(35) (a) Marder, S. R.; Perry, J. W.; Schaefer, W. P. *J. Mater. Chem.* **1992**, *2*, 985. (b) Marder, S. R.; Perry, J. W.; Schaefer, W. P. *Science* **1989**, *245*, 626. (c) Aakeroy, C. B.; Hitchcock, P. B.; Moyle, B. D.; Seddon, K. R. *J. Chem. Soc., Chem. Commun.* **1989**, 1856. (d) Aakeroy, C. B.; Azoz, N.; Calvert, P. D.; Kadim, M.; McCaffery, A. J.; Seddon, K. R. In *Materials for Nonlinear Optics: Chemical Perspectives*; Marder, S. R., Sohn, J. E., Stucky, G. D., Eds.; American Chemical Society: Washington, DC, 1991; Chapter 34, pp 516–527. (e) Aakeroy, C. B.; Hitchcock, P. B.; Seddon, K. R. *J. Chem. Soc., Chem. Commun.* **1992**, 553.

(36) Russell, V. A.; Etter, M. C.; Ward, M. D., manuscript in preparation.